

Hierarchical Contrastive Motion Learning for Video Action Recognition

Xitong Yang¹

xyang35@cs.umd.edu

Xiaodong Yang²

<https://xiaodongyang.org>

Sifei Liu²

<https://www.sifeiliu.net>

Deqing Sun³

<https://deqings.github.io>

Larry Davis¹

lsd@umiacs.umd.edu

Jan Kautz²

<https://jankautz.com>

¹ University of Maryland, College Park

² NVIDIA

³ Google

Abstract

One central question for video action recognition is how to model motion. In this paper, we present hierarchical contrastive motion learning, a novel self-supervised learning framework to extract effective motion representations from raw video frames. Our approach progressively learns a hierarchy of motion features that correspond to different abstraction levels in a network. At each level, an explicit motion self-supervision is provided via contrastive learning to enforce the motion features to capture semantic dynamics and evolve more discriminative for video action recognition. This hierarchical design bridges the semantic gap between low-level movement cues and high-level recognition tasks, and promotes the fusion of appearance and motion information at multiple levels. Our motion learning module is lightweight and flexible to be embedded into various backbone networks. Extensive experiments on four benchmarks show that the proposed approach consistently achieves superior results.

1 Introduction

Motion provides abundant and powerful cues for understanding the dynamic visual world. A broad range of video understanding tasks benefit from the introduction of motion information, such as action recognition [50, 59], activity detection [17, 68], object tracking [11, 68], etc. Thus, how to extract and model motion is one of the fundamental problems in video understanding. While early methods in this field mostly rely on the pre-computed motion features such as optical flow, recent works have been actively exploiting convolutional neural networks (CNNs) for more effective motion learning from raw video frames [42, 60], encouraged by the success of end-to-end learning in various vision tasks.

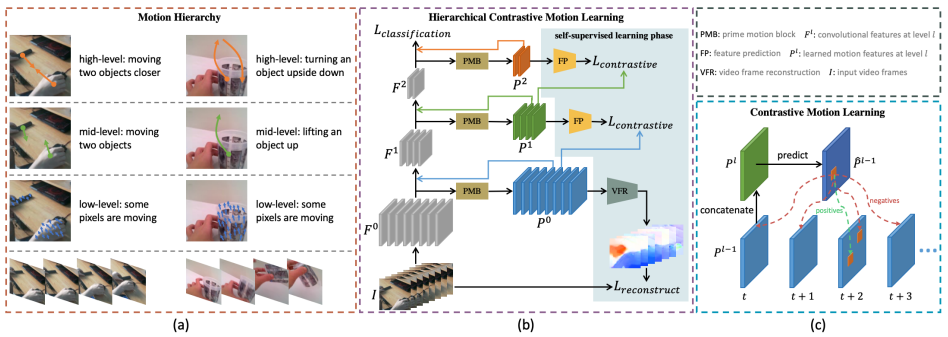


Figure 1: (a) Illustration of the hierarchy of progressively learned motion: from pixel-level and short-range movement to semantic temporal dynamics. (b) Architecture of the proposed motion learning module embedded in a backbone network. (c) Overview of positive and negative sampling for hierarchical contrastive learning to adopt higher-level motion features to predict future ones at lower-level.

A key challenge for end-to-end motion representation learning is to design an effective supervision. Unlike many other tasks that afford plenty of well-defined annotations, the “ground truth motion” is often unavailable or even undefined for motion learning in practice. One popular idea is to extract motion features by means of the action recognition supervision. However, the classification loss is shown to be sub-optimal in this task as it only provides an implied supervision to guide motion learning [63]. This supervision is also prone to be biased towards appearance information since some video action benchmarks can be mostly solved by considering static images without temporal modeling [49]. Recently, some efforts have been made to explore pretext tasks with direct supervisions for motion learning, such as optical flow prediction [62] and video frame reconstruction [74]. Although having shown promising results, such supervisions are restricted to pixel-wise and short-term motion as they hinge on pixel photometric loss and movement between adjacent frames.

In light of the above observations, we introduce a novel self-supervised learning framework that enables explicit motion supervision at multiple feature abstraction levels, which we term hierarchical contrastive motion learning. Specifically, given preliminary motion cues as a bootstrap, our approach progressively learns a hierarchy of motion features in a bottom-up manner, as illustrated in Figure 1(a). This hierarchical design is proposed to bridge the semantic gap between the low-level preliminary motion and the high-level recognition task—analogueous to the findings in neuroscience that humans perceive motion patterns in a hierarchical way [11, 14]. At each level, a discriminative contrastive loss [5, 19] is used to provide an explicit self-supervision to enforce the motion features at current level to predict the future ones at previous level. In contrast to the previous pretext tasks that focus on low-level image details, the contrastive learning encourages the model to learn useful semantic dynamics from previously learned motion features at a lower level, and is more favorable for motion learning at higher levels where the spatial and temporal resolutions of feature maps are low [9, 70, 14]. To acquire the preliminary motion cues to initialize the hierarchical motion learning, we exploit the video frame reconstruction [77, 48] as an auxiliary task such that the whole motion representation learning enjoys a unified self-supervised setup.

The proposed motion learning module is realized via a side network branch, which is lightweight and flexible to be embedded into a variety of backbone CNNs. As shown in Figure 1(b), the side branch (i.e., the shaded region) for self-supervised motion learning is

discarded after training, and only the learned motion features are retained in the form of residual connections [23]. Our hierarchical design also promotes the fusion of appearance and motion by integrating the motion features into the backbone network at multiple abstraction levels [10]. This multi-level fusion paradigm is unachievable for previous motion learning methods [0, 74] that depend solely on low-level motion supervisions.

We summarize our main contributions as follows. (1) We propose a new learning framework for motion representation learning from raw video frames. (2) We advance contrastive learning to a hierarchical design that bridges the semantic gap between low-level motion cues and high-level recognition tasks. (3) To our knowledge, this work provides the first attempt to empower contrastive learning in motion representation learning for large-scale video action recognition. (4) Our approach achieves superior results on four benchmarks without relying on off-the-shelf motion features or supervised pre-training.

2 Related Work

Action Recognition and Motion Extraction. A large family of video action research focuses on motion modeling [22, 39, 41, 50, 61, 64, 66, 67]. For example, the two-stream networks model temporal information by leveraging external motion inputs such as optical flow and frame differences [50, 61]. 3D CNNs [22, 64] and RNNs [41, 67] are also widely used to simultaneously model appearance and motion.

To learn more explicit motion representations, ActionFlowNet [42] uses pre-computed optical flow as an additional supervision to encode motion together with appearance, while D3D [53] tunes the spatial stream to predict the outputs of the temporal stream. However, these methods require the extraction of optical flow which is time consuming and infeasible for large-scale datasets. Recently, TVNet [9] proposes to formulate the TV-L1 algorithm [69] in a customized network layer, producing optical flow like motion features to complement static appearance. A differentiable representation flow layer is also developed in [49]. Inspired by the correlation layer in FlowNet [8], CorrNet [60] and MotionSqueeze [80] leverage the correlation operation to extract motion from convolutional features. All these studies employ classification loss as an indirect supervision or mimic optical flow design to learn motion extraction, while in this paper we aim to explicitly realize motion learning through the proposed hierarchical contrastive learning in a fully self-supervised way.

Self-Supervised Learning. To take advantage of the abundant unlabeled videos, numerous methods have been developed for video representation learning by different self-supervisory signals, such as frame interpolation [0, 76, 84, 83], sequence ordering [13, 31, 40], future prediction [37, 52, 63, 73]. While these methods do not require any pre-trained networks nor video annotations, the learned models tend to focus on low-level information and may not effectively catch the high-level and long-term temporal dynamics.

Contrastive learning has been recently explored for self-supervised learning of video representations [20, 21, 35, 46, 57, 65]. Several pretext tasks, such as future prediction [20, 35] and augmentation invariance [20, 65], are designed to facilitate learning of spatio-temporal representations that can benefit high-level video recognition tasks. In contrast to the existing work that focuses on self-supervised learning or model pretraining, our work leverages contrastive learning to extract motion information with an overall goal to improve supervised video classification. Moreover, we conduct contrastive motion learning at multiple levels across the hierarchical structure of a backbone network and present a progressive training strategy to build the higher-level motion from the well-learned lower-level ones.

3 Method

3.1 Overview

Given the convolutional features $\{\mathcal{F}^0, \dots, \mathcal{F}^{L-1}\}$ at different levels of a backbone network, our aim is to learn a **hierarchy** of motion representations $\{\mathcal{P}^0, \dots, \mathcal{P}^{L-1}\}$ for the corresponding levels. Here, L indicates the total number of abstraction levels. As the first step, we employ video frame reconstruction as the supervision to obtain the preliminary motion cues \mathcal{P}^0 , which function as a bootstrap for the following hierarchical motion learning. With that, we progressively learn the motion features in a bottom-up manner. At each level $l > 0$, we learn the motion features \mathcal{P}^l by enforcing them to predict the future motion features at the previous level $l - 1$, as described in Sec. 3.2. We use the contrastive loss as an objective such that \mathcal{P}^l is trained to capture semantic temporal dynamics from \mathcal{P}^{l-1} . The learned motion features at each level are integrated into a backbone network via residual connections to perform appearance and motion feature fusion: $\mathcal{Z}^l = \mathcal{F}^l + g^l(\mathcal{P}^l)$, where $g^l(\cdot)$ is used to match the feature dimensions. After learning motion at all levels, we jointly train the whole network for action recognition in a multi-tasking manner, as presented in Sec. 3.3.

3.2 Self-Supervised Motion Learning

Prime Motion Block. We first introduce a lightweight prime motion block (PMB) to transform the convolutional features of a backbone network to more discriminative representations for motion learning. The key component of this block is a cost volume layer, which is inspired by the success of using cost volumes in stereo matching [24] and optical flow estimation [59]. In our case, given a sequence of convolutional features $\mathcal{F} = \{F_0, \dots, F_{T-1}\}$ with length T , we first conduct an $1 \times 1 \times 1$ convolution to reduce the input channels by $1/\beta$, denoted as $\tilde{\mathcal{F}}$. This operation significantly reduces the computational overhead of prime motion block, and provides more compact representations to reserve the essential information to compute cost volumes. The adjacent features are then re-organized to feature pairs $\tilde{\mathcal{F}}^* = \{(\tilde{F}_0, \tilde{F}_1), \dots, (\tilde{F}_{T-2}, \tilde{F}_{T-1}), (\tilde{F}_{T-1}, \tilde{F}_{T-1})\}$, which are used to construct the cost volumes. The matching cost between two features is defined as:

$$\text{cv}_t(x_1, y_1, x_2, y_2) = \text{sim}(\tilde{F}_t(x_1, y_1), \tilde{F}_{t+1}(x_2, y_2)), \quad (1)$$

where $\tilde{F}_t(x, y)$ denotes the feature vector at time t and position (x, y) , and the cosine distance is used as the similarity function: $\text{sim}(u, v) = u^T v / \|u\| \|v\|$. We replicate the last feature map \tilde{F}_{T-1} to compute their cost volume in order to keep the original temporal resolution. We limit the search range with the max displacement of (x_2, y_2) to be d and use a striding factor s to handle large displacements without increasing the computation. As a result, the cost volume layer outputs a feature tensor of size $M \times H \times W$, where $M = (2 \times \lfloor d/s \rfloor + 1)^2$ and H, W denote the height and width of a feature map. It is noteworthy that computing cost volumes is lightweight as it has no learnable parameters and much fewer FLOPs than 3D convolutions. Finally, we combine the cost volumes with the features obtained after dimension reduction, motivated by the observation that the two features provide complementary information for localizing motion boundaries. We present more details of the prime motion block in the supplementary material.

Preliminary Motion Cues. Although the prime motion block extracts rough motion features from convolutional features, we find that such features are easily biased towards appear-

ance when jointly trained with the backbone network. Thus, an **explicit** motion supervision is vital for more effective motion learning at each level.

To initialize the progressive training, the preliminary motion cues, i.e., \mathcal{P}^0 , are required as a bootstrap. They should encode some low-level but valid movement information to facilitate the following motion learning. Therefore, we adopt video frame reconstruction to guide the extraction of preliminary motion cues. This task can be formulated as a self-supervised optical flow estimation problem [27, 48], aiming to produce optical flow to allow frame reconstruction from neighboring frames. Motivated by the success of recent work on estimating optical flow with CNNs [55], we build a simple optical flow estimation module using 5 convolutional layers with dense connections. We make use of the estimated optical flow to warp video frames through bilinear interpolation. The loss function consists of a photometric term that measures the error between the warped frame and the target frame, and a smoothness term that is used to handle the aperture problem that causes ambiguity in motion estimation: $\mathcal{L}_{\text{reconstruct}} = \mathcal{L}_{\text{photometric}} + \zeta \mathcal{L}_{\text{smoothness}}$. We define the photometric error as:

$$\mathcal{L}_{\text{photometric}} = \frac{1}{HWT} \sum_{t=1}^T \sum_{x=1}^W \sum_{y=1}^H \mathbb{1} \rho(I_t(x, y) - \hat{I}_t(x, y)), \quad (2)$$

where \hat{I}_t indicates the warped frame at time t and $\rho(z) = (z^2 + \varepsilon^2)^\alpha$ is the generalized Charbonnier penalty function with $\alpha = 0.45$ and $\varepsilon = 1e^{-3}$ [54], and the indicator function $\mathbb{1} \in \{0, 1\}$ is applied to exclude those invalid positions of the warped pixels that are out-of-boundary. Additionally, we compute the smoothness term as:

$$\mathcal{L}_{\text{smoothness}} = \frac{1}{T} \sum_{t=1}^T \rho(\nabla_x U_t) + \rho(\nabla_y U_t) + \rho(\nabla_x V_t) + \rho(\nabla_y V_t), \quad (3)$$

where $\nabla_x U/V$ and $\nabla_y U/V$ are the gradients of estimated flow fields U/V in x/y directions.

Hierarchical Motion Learning. Given above preliminary motion cues as a bootstrap, we propose to learn higher-level motion representations using a multi-level self-supervised objective based on the contrastive loss [6, 48, 49]. Our goal is to employ the higher-level motion features as a conditional input to guide the prediction of the future lower-level motion features that are well-learned from a previous step. By this way, the higher-level features are forced to understand a more abstract trajectory that summarizes motion dynamics from the lower-level ones. This objective therefore allows us to extract slowly varying features that progressively correspond to high-level semantic concepts [20, 44, 70].

Formally, let us denote the motion features generated by the prime motion block at level $l > 0$ as $\mathcal{P}^l = \{P_0^l, \dots, P_{T-1}^l\}$, where T indicates the sequence length. In order to train \mathcal{P}^l , we enforce P_t^l to predict the future motion features at the previous level (i.e., $P_{t+\delta}^{l-1}$), conditioned on the motion feature at the start time P_t^{l-1} , as illustrated in Figure 1(c). In practice, a predictive function f_δ is applied for the motion feature prediction at time step $t + \delta$: $\hat{P}_{t+\delta}^{l-1} = f_\delta([P_t^l, P_t^{l-1}])$, where $[\cdot, \cdot]$ denotes channel-wise concatenation. We employ a multi-layer perception (MLP) with one hidden layer as the prediction function: $f_\delta(x) = W_\delta^{(2)} \sigma(W_\delta^{(1)} x)$, where σ is ReLU and $W_\delta^{(1)}$ is shared across all prediction steps in order to leverage their common information. We define the objective function of each level as a contrastive loss, which encourages the predicted \hat{P}^{l-1} to be close to the ground truth P^{l-1} while being far away from the negative samples:

$$\mathcal{L}_{\text{contrastive}}^l = - \sum_{i \in \mathcal{S}} \left[\log \frac{\exp(\text{sim}(\hat{P}_i^{l-1}, P_i^{l-1})/\tau)}{\sum_{j \in \mathcal{S}} \exp(\text{sim}(\hat{P}_i^{l-1}, P_j^{l-1})/\tau)} \right], \quad (4)$$

where the similarity function is defined as the cosine similarity as the one used in computing cost volumes, and \mathcal{S} denotes the sampling space of positive and negative samples.

As shown in Figure 1(c), the positive sample of the predicted feature is the ground-truth feature that corresponds to the same video and locates at the same position in both space and time as the predicted one. Similar to [20], we define three types of negative samples for all prediction and ground-truth pairs: spatial negatives, temporal negatives and easy negatives. Considering efficiency, we randomly sample N spatial locations for each video within a mini-batch to compute the loss. See the supplementary material for more sampling details. As illustrated in Figure 1(b), the contrastive motion learning is performed for multiple levels until the motion hierarchy of the whole network is built up.

Progressive Training. Training the multi-level self-supervised learning framework simultaneously from the beginning is infeasible, as the lower-level motion features are initially not well-learned and the higher-level prediction would be arbitrary. To facilitate the optimization process, we propose a progressive training strategy that learns motion features for one level at a time, propagating from low-level to high-level. In practice, after the convergence of training at level $l - 1$, we freeze all network parameters up to level $l - 1$ (therefore fixing the motion features \mathcal{P}^{l-1}), and then start the training for level l . In this way, the higher-level motion features can be stably trained with the well-learned lower-level ones.

3.3 Joint Training for Action Recognition

Our ultimate goal is to improve video action recognition with the learned hierarchical motion features. To integrate the learned motion features into a backbone network, we wrap our prime motion block into a residual block: $\mathcal{Z}^l = \mathcal{F}^l + g^l(\mathcal{P}^l)$, where \mathcal{F}^l is the convolutional features at level l , \mathcal{P}^l is the corresponding motion features obtained in Sec. 3.2, and $g^l(\cdot)$ is a $1 \times 1 \times 1$ convolution. This seamless integration enables end-to-end fusion of appearance and motion information over multiple levels throughout a single unified network, instead of learning them disjointly like two-stream networks [50]. After the motion representations are self-supervised learned at all levels, we add in the classification loss to jointly optimize the total objective, which is a weighted sum of the following losses:

$$\mathcal{L}_{\text{total}} = \mathcal{L}_{\text{classification}} + \lambda \mathcal{L}_{\text{reconstruct}} + \sum_l \gamma^l \mathcal{L}_{\text{contrastive}}, \quad (5)$$

where λ and γ^l are the weights to balance related loss terms. As illustrated in Figure 1(b), our multi-level self-supervised learning is performed through a side network branch, which can be flexibly embedded into standard CNNs. Furthermore, this self-supervised learning side branch is discarded after training so that our final network can well maintain the efficiency at runtime for inference.

4 Experiments

We extensively evaluate our proposed approach on four benchmarks: Kinetics-400 [2], Something-Something (V1&V2) [18] and UCF-101 [51]. Our motion learning module is generic and can be instantiated with various video networks [2, 58, 62]. In our experiments, we use the standard networks R2D [62] and R(2+1)D [58] as our backbones. We follow the standard recipe in [2] for model training. Note that all models are trained from scratch

Input	Supervision			Score
	Action	Reconstruction	Contrastive	
Level 1	✓	✓		2.3
			✓	3.1
				–
Level 2	✓	✓		1.7
			✓	2.5
				3.0
Level 3	✓	✓		2.4
			✓	1.7
				3.0

Table 1: Comparison of efficacy scores of the motion features learned at different levels under different supervisory forms.

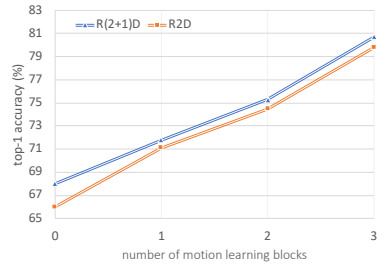


Figure 2: Comparison of the top-1 accuracy on UCF-101 with incrementally adding the proposed motion learning blocks.

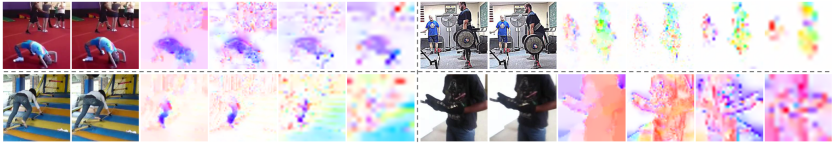


Figure 3: Visualization of the estimated optical flow at different feature abstraction levels. For each group, columns 1-2 are adjacent frames; column 3 is the reference optical flow extracted by [63]; columns 4-6 are the estimated optical flow at levels 1, 2 and 3.

or self-supervised pre-trained without additional annotations or pre-computed optical flow. More details on datasets and implementations are available in the supplementary material.

4.1 Ablation Study

Supervision for Motion Learning. We first compare the motion features learned at different levels by different supervisions. As our motion learning is based on the self-supervisions that are not directly related with the final action recognition, we first define a measurement to reflect the efficacy of the learned motion features. Towards this goal, we take the extracted motion feature as input and train a lightweight classifier for action recognition on UCF-101. We define the efficacy score as: $\text{Score} = \text{Acc}_{\text{train}} / (\text{Acc}_{\text{train}} - \text{Acc}_{\text{test}})$, where $\text{Acc}_{\text{train}}$ and Acc_{test} indicate the top-1 accuracy on the training and test sets. Intuitively, a higher score implies that the representation is more discriminative (with higher training accuracy) and generalizes better (with a lower performance gap between training and testing).

Table 1 shows the efficacy scores of motion features at different levels with different supervisions, where “action” indicates the supervision by action classification, and “reconstruction” and “contrastive” refer to the supervisions by frame reconstruction and contrastive learning. Levels 1, 2 and 3 correspond to the motion features extracted after res_2 , res_3 and res_4 of R2D. We observe that the self-supervision of low-level frame reconstruction is particularly effective at level 1, but its performance degrades dramatically at higher levels due to lower spatial/temporal resolutions and higher abstraction of convolutional features. In contrast, the proposed self-supervision by hierarchical contrastive learning is more stable over different levels and more effective to model motion dynamics. It is also observed that the self-supervision, with correct choices at different levels, consistently outperforms the supervision by action classification, which is consistent with the findings in [0, 40, 63]. In Figure 3, we visualize the estimated optical flow, the by-product of frame reconstruction at

Methods	PMB	Self-Sup	FLOPs	UCF-101	Something-V1	Kinetics-400
Baseline: R2D			1.00×	66.0 / 86.0	36.1 / 68.1	64.8 / 85.1
Ours: R2D	✓		1.18×	71.6 / 89.7	43.6 / 74.7	65.6 / 85.5
Ours: R2D	✓	✓	1.18×	79.8 / 94.4	44.3 / 75.8	67.3 / 86.4
Baseline: R(2+1)D			1.00×	68.0 / 88.2	48.5 / 78.1	66.8 / 86.6
Ours: R(2+1)D	✓		1.11×	73.4 / 92.1	49.2 / 77.9	67.4 / 86.9
Ours: R(2+1)D	✓	✓	1.11×	80.7 / 95.6	50.4 / 78.9	68.3 / 87.4

Table 2: Ablation study on the prime motion block (PMB) and self-supervision (Self-Sup) for action recognition. We report the computational cost and top-1 / top-5 accuracy (%) on the three benchmarks. Models are evaluated using a single clip per video to eliminate the impact of test-time augmentation.

each level, and find that more accurate optical flow indeed presents at lower levels.

Contributions of Individual Components. We verify the contributions of the proposed components in Table 2. It is obvious that our approach consistently and significantly improves the action recognition accuracy for both 2D and 3D action networks. Our prime motion block provides complementary motion features at multiple levels, and the self-supervision further enhances the representations to encode semantic dynamics. In particular, for the dataset that heavily depends on temporal information like Something-V1, our approach remarkably improves the performance of baseline R2D by 8.2%. For the dataset that is small-scale and tends to overfit to the appearance information like UCF-101, our method improves model generalization and achieves 13.8% improvement. Moreover, our motion learning module only introduces a small overhead to FLOPs of the backbone network.

We next validate the contribution of our motion learning at each level by incrementally adding the proposed motion feature learning block to the baseline. Figure 2 demonstrates the results based on the backbones of R2D and R(2+1)D on UCF-101. We observe that notable gains can be obtained at multiple levels, and the performance gain does not vanish with the increase of motion learning blocks, suggesting the importance of leveraging hierarchical motion information across all levels.

4.2 Comparison with State-of-the-Art Results

We compare our approach with the state-of-the-art methods on the four action recognition benchmarks. We report results with the standard test-time augmentations [47]: increasing the spatial resolution to 256×256 and sampling multiple clips per video (9 clips for Something-V1&V2 and 30 clips for Kinetics-400).

Table 3 shows the comparisons on Kinetics-400 and Something-V1&V2. Without using optical flow or supervised pre-training, our model based on backbone R(2+1)D-101 achieves the best results among the single-stream methods over all three datasets. Our approach also outperforms most two-stream methods, apart from the recent two-stream TSM [47] on Something-V2. As for the datasets that focus more on temporal modeling like Something-V1&V2, 2D networks are usually not able to achieve as good results as 3D models. However, by equipping with the proposed motion learning module, we find that our method based on backbone R2D-50 outperforms some 3D models, such as R(2+1)D and NL I3D. Our approach also achieves superior results compared with the most recent work that are specifically designed for temporal motion modeling (i.e., the second group in Table 3). More importantly, our motion learning is fully self-supervised from raw video frames without any supervisions from optical flow or pre-trained temporal stream.

Methods	Pre-Training	Two-Stream	Kinetics-400	Something-V1	Something-V2
I3D [10]	ImageNet	✓	75.7	—	—
R(2+1)D [38]	Sports1M	✗	74.3	45.7	—
R(2+1)D [38]	Sports1M	✓	75.4	—	—
NL I3D-50 [16]	ImageNet	✗	76.5	44.4	—
S3D-G [39]	ImageNet	✓	77.2	48.2	—
TRN [40]	ImageNet	✓	—	42.0	55.5
TSM [41]	ImageNet	✗	75.7	49.7	63.4
TSM [42]	ImageNet	✓	—	52.6	66.0
ECO [43]	✗	✓	70.0	49.5	—
SlowFast [44]	✗	✗	77.9	—	—
Disentangling [45]	ImageNet	✗	71.5	—	—
D3D [46]	ImageNet	✗	75.9	—	—
STM [47]	ImageNet	✗	73.7	50.7	64.2
Rep. Flow [48]	✗	✗	77.1	—	—
MARS [9]	✗	✗	72.7	—	—
DynamoNet [9]	✗	✗	77.9	—	—
Ours, R2D-50	✗	✗	74.8	46.2	59.4
Ours, R(2+1)D-101	✗	✗	78.3	52.8	64.4

Table 3: Comparison of the top-1 accuracy (%) with the state-of-the-art methods on Kinetics-400 and Something-V1&V2.

Method	Dataset	Accuracy
Shuffle and Learn [49]	UCF-101	50.2
OPN [50]	UCF-101	59.8
Odd-One-Out [51]	UCF-101	60.3
ActionFlowNet* [52]	UCF-101	83.9
3D-Puzzle [53]	Kinetics-400	65.8
DPC [54]	Kinetics-400	75.7
DynamoNet [9]	YouTube8M	88.1
Ours: R2D-50 (random)	—	69.9
Ours: R2D-50	Kinetics-400	82.2
Ours: R(2+1)D-101 (random)	—	70.9
Ours: R(2+1)D-101	Kinetics-400	85.1

Table 4: Comparison of the top-1 accuracy (%) with self-supervised methods on UCF-101 (split-1).

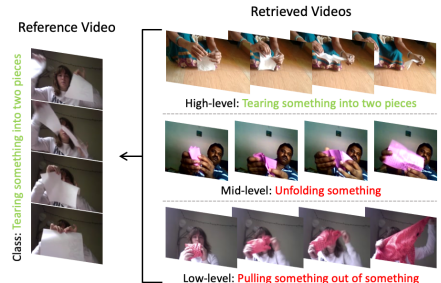


Figure 4: Examples of the retrieved videos to reflect the different motion semantics learned by the motion features at different levels.

4.3 More Analysis

Self-Supervised Pre-Training. The self-supervised learning of video representations has been gaining increasing attention in recent years [10, 16, 20, 29, 31, 40]. In addition to hierarchical motion learning, our multi-level self-supervised learning can also serve as pre-training of a network. As an example, after self-supervised pre-training on Kinetics-400 (without using its action labels), we fine-tune the network on UCF-101 for action recognition. We compare our approach with other state-of-the-art self-supervised methods in Table 4. Interestingly, even though not specifically designed for network pre-training, our approach is capable of learning effective video representation that generalizes well to the small dataset. Note that previous work requires optical flow [42] or a much larger pre-training dataset (YouTube8M) [9] to achieve state-of-the-art results.

Motion at Different Levels. Here we investigate the different semantics integrated in the motion features learned at different levels. This can be justified by the following observations. We conduct a video retrieval experiment and find that compared to the motion features at higher levels, the ones at lower levels tend to retrieve the videos sharing similar elementary movements but lacking of high-level action correlation, as illustrated in Figure 4. More analysis is available in the supplementary material.

5 Conclusion

We have presented hierarchical contrastive motion learning, a multi-level self-supervised framework that progressively learns a hierarchy of motion features from raw video frames. A discriminative contrastive loss at each level provides explicit self-supervision for motion learning. This hierarchical design bridges the semantic gap between low-level motion cues and high-level recognition tasks, meanwhile promotes effective fusion of appearance and motion information to finally boost action recognition. Extensive experiments on four benchmarks show that our approach compares favorably against the state-of-the-art methods yet without requiring optical flow or supervised pre-training.

Appendix

Section A presents additional experiments to (1) compare the differences of the motion features learned at different levels, (2) evaluate the transferability of our learned features to UCF-101, and (3) report the computational cost of our approach. Section B shows qualitative results using Grad-CAM++. Sections C and D respectively provide more details of our approach as well as the training on each specific dataset.

A Additional Experimental Results

A.1 Motion at different levels

To study the different semantics encoded in the motion features learned at different levels, we report several observations including a video retrieval experiment performed in Section 4.3 of the paper. Here we extend this experiment and conduct an additional video classification experiment directly using the learned motion features of different levels to further compare the different semantics embedded in the motion features. Specifically, we use the k-nearest-

	Acc (%)	Classes with the largest relative gains
Low-level	11.6	“turning the camera left” (73.8)
		“turning the camera right” (71.7)
		“turning the camera upwards” (58.3)
Mid-level	15.2	“showing a photo to the camera” (0 → 19.4)
		“showing smth behind smth” (0 → 12.2)
		“poking a stack of smth” (0 → 9.5)
High-level	21.7	“pulling two ends of smth” (0 → 14.0)
		“tipping smth with smth in it over” (0 → 12.5)
		“sprinkling smth onto smth” (0 → 9.1)

Table 5: Comparison of classification accuracy using motion features learned at different levels (accuracy for random output: 0.6%). For the mid/high levels, we show the top-3 classes with the largest relative gains compared with the lower-level motion features. For the low level, we report the top-3 classes with the highest accuracy instead.

Method	Flow	GFLOPs×Crops	Top-1	Top-5
I3D [10]		108 × N/A	72.1	90.3
I3D [10]	✓	216 × N/A	75.7	92.0
S3D-G [54]	✓	143 × N/A	77.2	93.0
NL I3D-50 [52]		282 × 30	76.5	92.6
NL I3D-101 [52]		359 × 30	77.7	93.3
R(2+1)D [53]		152 × 115	74.3	91.4
R(2+1)D [53]	✓	304 × 115	75.4	91.9
Ours , R2D		49 × 30	74.8	91.6
Ours , R(2+1)D		150 × 30	78.3	93.3

Table 6: Comparison of computational cost and top-1 / top-5 accuracy on Kinetics-400.

Methods	Pre-Training	UCF-101
I3D [10]	ImageNet + Kinetics-400	95.4
R(2+1)D [53]	Kinetics-400	96.8
S3D-G [54]	ImageNet + Kinetics-400	96.8
Disentangling [14]	ImageNet + Kinetics-400	95.9
D3D [52]	ImageNet + Kinetics-400	97.0
STM [43]	ImageNet + Kinetics-400	96.2
MARS [8]	Kinetics-400	97.0
DynamoNet [9]	YouTube8M + Kinetics-400	97.8
Ours , R(2+1)D-101	Kinetics-400	97.8

Table 7: Comparison of top-1 accuracy (%) with the state-of-the-art methods on UCF-101.

neighbor (KNN) for video classification. Given a query video, we first rank the videos in the validation set based on the ℓ_2 distance of their motion features extracted at a certain level, and then assign the query video to the majority class among its top k nearest neighbors.

We compare the classification accuracy for motion features learned at different levels in Table 5. It is not surprising that the motion features at higher levels achieve higher accuracy than the ones at lower levels as the former possess more useful semantics of motion dynamics for the video action recognition task. More interestingly, we find that the low-level motion features can obtain relatively high accuracy for some action classes with apparent moving patterns (e.g., “turning the camera left”). This indicates that the low-level motion features are capable of extracting elementary movements from raw video frames. On the other hand, the motion features at higher levels can recognize the actions that require finer understanding of high-level motion semantics (e.g., “pulling two ends of something so that it separates into two pieces”). This finding validates the motion hierarchy illustrated in Figure 1 of the paper.

A.2 Transferring to UCF-101

To demonstrate the transferability of our learned features to smaller-scale datasets, we fine-tune the pre-trained model on UCF-101. Specifically, our models is pre-trained on Kinetics-400 only for classification following the standard setting in previous work [10, 53], and we report the average accuracy over all 3 splits on UCF-101. As shown in Table 7, our approach achieves 97.8% top-1 accuracy, a new state-of-the-art result among the single-stream methods on UCF-101.

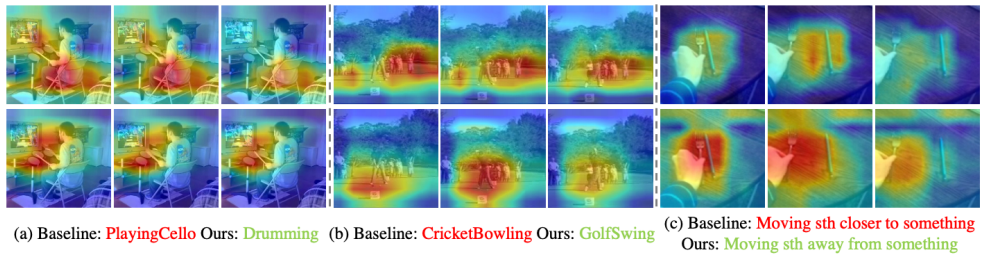


Figure 5: Visualization of the learned features by Grad-CAM++ [4]. Fonts in green and red indicate correct recognition and misclassification. (a-b) Features learned by our approach (bottom) are more sensitive to the regions with important motion cues. (c) Our motion learning module (bottom) equips the 2D backbone with the ability of reasoning the temporal order of video frames.

A.3 Computational Cost

Our motion representation learning module is flexible to plug in a standard network and only introduces a small computation overhead to the backbone. We compare the computational cost in GFLOPs of our models with the state-of-the-art methods in Table 6. As the computational cost is highly affected by the backbone architecture, we only show the methods using similar backbone networks as our approach for fair comparisons. It can be observed that our models achieve superior results while maintaining a low inference-time cost, especially compared with the methods using two-stream networks.

B Qualitative Result

To qualitatively verify the impact of the learned motion features, we utilize Grad-CAM++ [4] to visualize the class activation map of the last convolution layer. Figure 5 shows the comparison between baseline and our model with the backbone R2D-50 on UCF-101 and Something-V1. Our model attentions more on the regions with informative motion, while the baseline tends to be distracted by the static appearance. For instance, in Figure 5(a), our method focuses on the moving hands of the person, while the baseline concentrates on the static human body. Our motion learning module also equips the 2D backbone with effective temporal modeling ability. As shown in Figure 5(c), our model is capable of reasoning the temporal order of the video and predicting the correct action, while the baseline outputs the opposite prediction result as it fails to capture the chronological relationship.

C Model Details

C.1 Backbones

We adopt the standard convolutional networks R2D-50 [62] and R(2+1)D-101 [68] as the backbones used in our experiments. A few changes are made to improve the computation efficiency, as demonstrated in Table 8. Compared with the original network R(2+1)D-101, our backbone supports higher input resolution and applies bottleneck layers with consistent number of channels. We start temporal striding from res_3 rather than res_4 , and employ the

Layer	R2D-50 / R(2+1)D-101	Output Size
input	—	$T \times 224 \times 224$
conv ₁	$1 \times 7 \times 7, 64$ stride: $1 \times 2 \times 2$	$T \times 112 \times 112$
res ₂	$\begin{bmatrix} 1 \times 1 \times 1, 64 \\ 1 \times 3 \times 3, 64 \\ 1 \times 1 \times 1, 256 \end{bmatrix} \times 3$	$T \times 56 \times 56$
res ₃	$\begin{bmatrix} 1 \times 1 \times 1, 128 \\ 1 \times 3 \times 3, 128 \\ 1 \times 1 \times 1, 512 \end{bmatrix} \times 4$	$T/2 \times 28 \times 28$
res ₄	$\begin{bmatrix} 1 \times 1 \times 1, 256 \\ (3 \times 1 \times 1, 256) \\ 1 \times 3 \times 3, 256 \\ 1 \times 1 \times 1, 1024 \end{bmatrix} \times 6 / 23$	$T/4 \times 14 \times 14$
res ₅	$\begin{bmatrix} 1 \times 1 \times 1, 512 \\ (3 \times 1 \times 1, 512) \\ 1 \times 3 \times 3, 512 \\ 1 \times 1 \times 1, 2048 \end{bmatrix} \times 3$	$T/4 \times 7 \times 7$

Table 8: Details of the architectures of the backbone networks R2D-50 / R(2+1)D-101 used in our experiments.

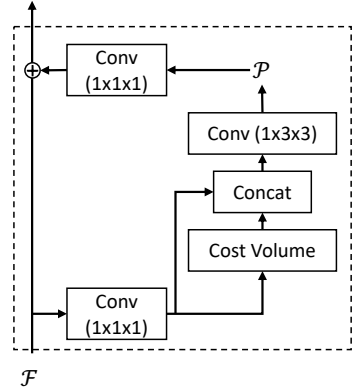


Figure 6: Architecture of PMB. \mathcal{F} and \mathcal{P} denote the convolutional feature from backbone network and the extracted motion feature, respectively.

top-heavy design as used in [64] for R(2+1)D-101, i.e., only using temporal convolutions in res₄ and res₅.

C.2 Prime Motion Block

Here we describe the prime motion block in more details. As illustrated in Figure 6, the prime motion block is wrapped as a residual block [23] such that the motion features \mathcal{P} can be inserted into a backbone network seamlessly. For the cost volume layer, we limit the search range with the maximum displacement $d = 6$ and the stride $s = 2$, which is equivalent to covering a region of 13×13 pixels with a stride 2. To combine the complementary information provided by the cost volumes and the convolutional features (after dimension reduction), we concatenate the two features in channels and then perform a 2D convolution. We use batch normalization [25] and ReLU after each convolutional layer and cost volume layer.

C.3 Sampling Strategy

We denote the predicted motion feature at level l as $\hat{P}_{t,k}^l$, where $t \in \{1, \dots, T^l\}$ is the temporal index, and $k \in \{(1,1), (1,2), \dots, (H^l, W^l)\}$ is the spatial index. The only positive pair is $(\hat{P}_{t,k}^l, P_{t,k}^l)$, which is the ground-truth feature that corresponds to the same video and locates at the same position in both space and time as the predicted one. Following the terminology used in [20], we define three types of negative samples for all the prediction and ground-truth pairs $(\hat{P}_{t,k}^l, P_{t,m}^l)$:

Spatial negatives are the ground-truth features that come from the same video of the predicted one but at a different spatial position, i.e., $k \neq m$. Considering the efficiency, we randomly sample N spatial locations for each video within a mini-batch to compute the loss. So the number of spatial negatives is $(N - 1)T^l$.

Temporal negatives are the ground-truth features that come from the same video and same spatial position, but from different time steps, i.e., $k = m, t \neq \tau$. They are the hardest negative samples to classify, and the number of temporal negatives are $T^l - 1$.

Easy negatives are the ground-truth features that come from different videos, and the number of easy negatives are $(B - 1)NT^l$, where B is the batch size.

D Experimental Details

D.1 Datasets

We extensively evaluate our proposed approach on the four benchmarks: Kinetics-400 [4], Something-Something (V1&V2) [16] and UCF-101 [5]. **Kinetics-400** is a large-scale video dataset with 400 action categories. As some videos are deleted by their owners over time, our experiments are conducted on a subset of the original dataset with approximately 238K training videos ($\sim 96\%$) and 196K validation videos ($\sim 98\%$). In practice, we notice a bit accuracy drop for the same model using our collected dataset with fewer training samples, suggesting that our results can be further improved with the full original dataset. **Something-Something (V1&V2)** are more sensitive to temporal motion modeling. Something-V1 contains about 100K videos covering 174 classes, and Something-V2 increases videos to 221K and improves video resolution and annotation quality. **UCF-101** includes about 13K videos with 101 classes. As the number of training videos is small, it is often used for evaluating unsupervised representation learning [4, 42] and transfer learning [47, 53].

D.2 Implementation details

We use the synchronized SGD with a cosine learning rate scheduling [36] and a linear warm-up [15] for all model training. The spatial size of the input is 224×224 , randomly cropped and horizontally flipped from a scaled video with the shorter side randomly sampled in [256, 320] pixels for R2D-50, and [256, 340] pixels for R(2+1)D-101. We apply temporal jittering when sampling clips from a video. The balancing weights for the joint training in Eq. (5) are set to $\lambda = 15, \gamma^1 = \gamma^2 = 0.25$, respectively. We describe the training details for different benchmarks as follow.

Kinetics-400. We sample a clip of $T = 16$ frames with a temporal stride 2 for the experiments using the backbone R2D-50 and $T = 32$ frames for those with the backbone R(2+1)D-101. We train all models using the distributed SGD on GPU clusters with 8 clips per GPU. We set the learning rate per GPU to 0.0025, and linearly scale the learning rate according to the number of GPUs. For the self-supervised training phase, all models are trained for 80 epochs with the first 10 epochs for warm-up, and the global batch normalization (BN) [25] is used to avoid trivial solution. As for the joint training phase, the models are trained for 200 epochs with the first 40 epochs for warm-up, and BN statistics is computed within each 8 clips.

Something-V1&V2. Since this dataset has a higher frame rate than Kinetics-400, we sample a clip of $T = 32$ frames with a temporal stride 1 for all experiments. Models are trained for 150 epochs with the first 50 epochs for warm-up and the learning rate per GPU is also 0.0025.

UCF-101. For the experiments described in Table 7 in the supplementary material, the models are initialized with the weights pre-trained on Kinetics-400 for classification, and then are fine-tuned for 30 epochs with a batch size of 32 and a learning rate of 0.002.

References

- [1] Johannes Bill, Hrag Pailian, Samuel J Gershman, and Jan Drugowitsch. Hierarchical structure is employed by humans during visual motion perception. *Journal of Vision*, 2019.
- [2] Joao Carreira and Andrew Zisserman. Quo vadis, action recognition? A new model and the kinetics dataset. In *CVPR*, 2017.
- [3] Aditya Chattopadhyay, Anirban Sarkar, Prantik Howlader, and Vineeth N Balasubramanian. Grad-CAM++: Improved visual explanations for deep convolutional networks. *arXiv:1710.11063*, 2017.
- [4] Ting Chen, Simon Kornblith, Mohammad Norouzi, and Geoffrey Hinton. A simple framework for contrastive learning of visual representations. In *ICML*, 2020.
- [5] Sumit Chopra, Raia Hadsell, and Yann LeCun. Learning a similarity metric discriminatively, with application to face verification. In *CVPR*, 2005.
- [6] Nieves Crasto, Philippe Weinzaepfel, Karteek Alahari, and Cordelia Schmid. MARS: Motion-augmented RGB stream for action recognition. In *CVPR*, 2019.
- [7] Ali Diba, Vivek Sharma, Luc Van Gool, and Rainer Stiefelhagen. DynamoNet: Dynamic action and motion network. In *ICCV*, 2019.
- [8] Alexey Dosovitskiy, Philipp Fischer, Eddy Ilg, Philip Hausser, Caner Hazirbas, Vladimir Golkov, Patrick Van Der Smagt, Daniel Cremers, and Thomas Brox. FlowNet: Learning optical flow with convolutional networks. In *ICCV*, 2015.
- [9] Lijie Fan, Wenbing Huang, Chuang Gan, Stefano Ermon, Boqing Gong, and Junzhou Huang. End-to-end learning of motion representation for video understanding. In *CVPR*, 2018.
- [10] Christoph Feichtenhofer, Axel Pinz, and Andrew Zisserman. Convolutional two-stream network fusion for video action recognition. In *CVPR*, 2016.
- [11] Christoph Feichtenhofer, Axel Pinz, and Andrew Zisserman. Detect to track and track to detect. In *ICCV*, 2017.
- [12] Christoph Feichtenhofer, Haoqi Fan, Jitendra Malik, and Kaiming He. SlowFast networks for video recognition. In *ICCV*, 2019.
- [13] Basura Fernando, Hakan Bilen, Efstratios Gavves, and Stephen Gould. Self-supervised video representation learning with odd-one-out networks. In *CVPR*, 2017.
- [14] Martin A Giese and Tomaso Poggio. Neural mechanisms for the recognition of biological movements. *Nature Reviews Neuroscience*, 2003.
- [15] Priya Goyal, Piotr Dollár, Ross Girshick, Pieter Noordhuis, Lukasz Wesolowski, Aapo Kyrola, Andrew Tulloch, Yangqing Jia, and Kaiming He. Accurate, large minibatch SGD: Training ImageNet in 1 hour. *arXiv:1706.02677*, 2017.

- [16] Raghav Goyal, Samira Ebrahimi Kahou, Vincent Michalski, Joanna Materzynska, Susanne Westphal, Heuna Kim, Valentin Haenel, Ingo Fruend, Peter Yianilos, and Moritz Mueller-Freitag. The “something something” video database for learning and evaluating visual common sense. In *ICCV*, 2017.
- [17] Chunhui Gu, Chen Sun, Sudheendra Vijayanarasimhan, Caroline Pantofaru, David A Ross, George Toderici, Yeqing Li, Susanna Ricco, Rahul Sukthankar, and Cordelia Schmid. AVA: A video dataset of spatio-temporally localized atomic visual actions. In *CVPR*, 2018.
- [18] Michael Gutmann and Aapo Hyvärinen. Noise-contrastive estimation: A new estimation principle for unnormalized statistical models. In *AISTATS*, 2010.
- [19] Raia Hadsell, Sumit Chopra, and Yann LeCun. Dimensionality reduction by learning an invariant mapping. In *CVPR*, 2006.
- [20] Tengda Han, Weidi Xie, and Andrew Zisserman. Video representation learning by dense predictive coding. In *ICCV Workshop*, 2019.
- [21] Tengda Han, Weidi Xie, and Andrew Zisserman. Self-supervised co-training for video representation learning. *Advances in Neural Information Processing Systems*, 33, 2020.
- [22] Kensho Hara, Hirokatsu Kataoka, and Yutaka Satoh. Can spatiotemporal 3D CNNs retrace the history of 2D CNNs and ImageNet? In *CVPR*, 2018.
- [23] Kaiming He, Xiangyu Zhang, Shaoqing Ren, and Jian Sun. Deep residual learning for image recognition. In *CVPR*, 2016.
- [24] Asmaa Hosni, Christoph Rhemann, Michael Bleyer, Carsten Rother, and Margrit Gelautz. Fast cost-volume filtering for visual correspondence and beyond. *TPAMI*, 2012.
- [25] Sergey Ioffe and Christian Szegedy. Batch normalization: Accelerating deep network training by reducing internal covariate shift. In *ICML*, 2015.
- [26] Joel Janai, Fatma Guney, Anurag Ranjan, Michael Black, and Andreas Geiger. Unsupervised learning of multi-frame optical flow with occlusions. In *ECCV*, 2018.
- [27] J Yu Jason, Adam W Harley, and Konstantinos G Derpanis. Back to basics: Unsupervised learning of optical flow via brightness constancy and motion smoothness. In *ECCV*, 2016.
- [28] Boyuan Jiang, Mengmeng Wang, Weihao Gan, Wei Wu, and Junjie Yan. STM: Spatiotemporal and motion encoding for action recognition. In *ICCV*, 2019.
- [29] Dahun Kim, Donghyeon Cho, and Inso Kweon. Self-supervised video representation learning with space-time cubic puzzles. In *AAAI*, 2019.
- [30] Heeseung Kwon, Manjin Kim, Suha Kwak, and Minsu Cho. Motionsqueeze: Neural motion feature learning for video understanding. In *ECCV*, 2020.
- [31] Hsin-Ying Lee, Jia-Bin Huang, Maneesh Singh, and Ming-Hsuan Yang. Unsupervised representation learning by sorting sequences. In *ICCV*, 2017.

- [32] Ji Lin, Chuang Gan, and Song Han. TSM: Temporal shift module for efficient video understanding. In *ICCV*, 2019.
- [33] Ce Liu. *Beyond pixels: Exploring new representations and applications for motion analysis*. PhD thesis, MIT, 2009.
- [34] Gucan Long, Laurent Kneip, Jose M Alvarez, Hongdong Li, Xiaohu Zhang, and Qifeng Yu. Learning image matching by simply watching video. In *ECCV*, 2016.
- [35] Guillaume Lorre, Jaonary Rabarisoa, Astrid Orcesi, Samia Ainouz, and Stephane Canu. Temporal contrastive pretraining for video action recognition. In *The IEEE Winter Conference on Applications of Computer Vision*, pages 662–670, 2020.
- [36] Ilya Loshchilov and Frank Hutter. SGDR: Stochastic gradient descent with warm restarts. In *ICLR*, 2017.
- [37] William Lotter, Gabriel Kreiman, and David Cox. Deep predictive coding networks for video prediction and unsupervised learning. In *ICLR*, 2017.
- [38] Zhichao Lu, Vivek Rathod, Ronny Votel, and Jonathan Huang. RetinaTrack: Online single stage joint detection and tracking. In *CVPR*, 2020.
- [39] Behrooz Mahasseni, Xiaodong Yang, Pavlo Molchanov, and Jan Kautz. Budget-aware activity detection with a recurrent policy network. In *BMVC*, 2018.
- [40] Ishan Misra, C Lawrence Zitnick, and Martial Hebert. Shuffle and learn: unsupervised learning using temporal order verification. In *ECCV*, 2016.
- [41] Yue-Hei Ng, Matthew Hausknecht, Sudheendra Vijayanarasimhan, Oriol Vinyals, Rajat Monga, and George Toderici. Beyond short snippets: Deep networks for video classification. In *CVPR*, 2015.
- [42] Yue-Hei Ng, Jonghyun Choi, Jan Neumann, and Larry Davis. ActionFlowNet: Learning motion representation for action recognition. In *WACV*, 2018.
- [43] Simon Niklaus and Feng Liu. Context-aware synthesis for video frame interpolation. In *CVPR*, 2018.
- [44] Aaron Oord, Yazhe Li, and Oriol Vinyals. Representation learning with contrastive predictive coding. *arXiv:1807.03748*, 2018.
- [45] AJ Piergiovanni and Michael S Ryoo. Representation flow for action recognition. In *CVPR*, 2019.
- [46] Rui Qian, Tianjian Meng, Boqing Gong, Ming-Hsuan Yang, Huisheng Wang, Serge Belongie, and Yin Cui. Spatiotemporal contrastive video representation learning. *arXiv preprint arXiv:2008.03800*, 2020.
- [47] Zhaofan Qiu, Ting Yao, Chong-Wah Ngo, Xinmei Tian, and Tao Mei. Learning spatio-temporal representation with local and global diffusion. In *CVPR*, 2019.
- [48] Zhe Ren, Junchi Yan, Bingbing Ni, Bin Liu, Xiaokang Yang, and Hongyuan Zha. Unsupervised deep learning for optical flow estimation. In *AAAI*, 2017.

- [49] Laura Sevilla-Lara, Shengxin Zha, Zhicheng Yan, Vedanuj Goswami, Matt Feiszli, and Lorenzo Torresani. Only time can tell: Discovering temporal data for temporal modeling. *arXiv:1907.08340*, 2019.
- [50] Karen Simonyan and Andrew Zisserman. Two-stream convolutional networks for action recognition in videos. In *NeurIPS*, 2014.
- [51] Khurram Soomro, Amir Roshan Zamir, and Mubarak Shah. UCF101: A dataset of 101 human actions classes from videos in the wild. *arXiv:1212.0402*, 2012.
- [52] Nitish Srivastava, Elman Mansimov, and Ruslan Salakhudinov. Unsupervised learning of video representations using LSTMs. In *ICML*, 2015.
- [53] Jonathan C Stroud, David A Ross, Chen Sun, Jia Deng, and Rahul Sukthankar. D3D: Distilled 3D networks for video action recognition. In *WACV*, 2020.
- [54] Deqing Sun, Stefan Roth, and Michael J Black. A quantitative analysis of current practices in optical flow estimation and the principles behind them. *IJCV*, 2014.
- [55] Deqing Sun, Xiaodong Yang, Ming-Yu Liu, and Jan Kautz. PWC-Net: CNNs for optical flow using pyramid, warping, and cost volume. In *CVPR*, 2018.
- [56] Deqing Sun, Xiaodong Yang, Ming-Yu Liu, and Jan Kautz. Models matter, so does training: An empirical study of CNNs for optical flow estimation. *TPAMI*, 2019.
- [57] Li Tao, Xueting Wang, and Toshihiko Yamasaki. Self-supervised video representation learning using inter-intra contrastive framework. In *Proceedings of the 28th ACM International Conference on Multimedia*, MM ’20, page 2193–2201, New York, NY, USA, 2020. Association for Computing Machinery. ISBN 9781450379885. doi: 10.1145/3394171.3413694. URL <https://doi.org/10.1145/3394171.3413694>.
- [58] Du Tran, Heng Wang, Lorenzo Torresani, Jamie Ray, Yann LeCun, and Manohar Paluri. A closer look at spatiotemporal convolutions for action recognition. In *CVPR*, 2018.
- [59] Heng Wang and Cordelia Schmid. Action recognition with improved trajectories. In *ICCV*, 2013.
- [60] Heng Wang, Du Tran, Lorenzo Torresani, and Matt Feiszli. Video modeling with correlation networks. In *CVPR*, 2020.
- [61] Limin Wang, Yuanjun Xiong, Zhe Wang, Yu Qiao, Dahua Lin, Xiaoou Tang, and Luc Van Gool. Temporal segment networks: Towards good practices for deep action recognition. In *European conference on computer vision*, pages 20–36. Springer, 2016.
- [62] Xiaolong Wang, Ross Girshick, Abhinav Gupta, and Kaiming He. Non-local neural networks. In *CVPR*, 2018.
- [63] Junyuan Xie, Ross Girshick, and Ali Farhadi. Deep3D: Fully automatic 2D-to-3D video conversion with deep convolutional neural networks. In *ECCV*, 2016.
- [64] Saining Xie, Chen Sun, Jonathan Huang, Zhuowen Tu, and Kevin Murphy. Rethinking spatiotemporal feature learning: Speed-accuracy trade-offs in video classification. In *ECCV*, 2018.

- [65] Ceyuan Yang, Yinghao Xu, Bo Dai, and Bolei Zhou. Video representation learning with visual tempo consistency. *arXiv preprint arXiv:2006.15489*, 2020.
- [66] Xiaodong Yang, Pavlo Molchanov, and Jan Kautz. Multilayer and multimodal fusion of deep neural networks for video classification. In *ACM MM*, 2016.
- [67] Xiaodong Yang, Pavlo Molchanov, and Jan Kautz. Making convolutional networks recurrent for visual sequence learning. In *CVPR*, 2018.
- [68] Xitong Yang, Xiaodong Yang, Ming-Yu Liu, Fanyi Xiao, Larry Davis, and Jan Kautz. STEP: Spatio-temporal progressive learning for video action detection. In *CVPR*, 2019.
- [69] Christopher Zach, Thomas Pock, and Horst Bischof. A duality based approach for realtime TV-L1 optical flow. In *Joint Pattern Recognition Symposium*, 2007.
- [70] Zhang Zhang and Dacheng Tao. Slow feature analysis for human action recognition. *TPAMI*, 2012.
- [71] Yue Zhao, Yuanjun Xiong, and Dahua Lin. Recognize actions by disentangling components of dynamics. In *CVPR*, 2018.
- [72] Bolei Zhou, Alex Andonian, Aude Oliva, and Antonio Torralba. Temporal relational reasoning in videos. In *ECCV*, 2018.
- [73] Tinghui Zhou, Shubham Tulsiani, Weilun Sun, Jitendra Malik, and Alexei A Efros. View synthesis by appearance flow. In *ECCV*, 2016.
- [74] Yi Zhu, Zhenzhong Lan, Shawn Newsam, and Alexander Hauptmann. Hidden two-stream convolutional networks for action recognition. In *ACCV*, 2018.
- [75] Mohammadreza Zolfaghari, Kamaljeet Singh, and Thomas Brox. Eco: Efficient convolutional network for online video understanding. In *ECCV*, 2018.